Seismic inversion for reservoir facies under geologically realistic prior uncertainty with 3D convolutional neural networks

Anshuman Pradhan and Tapan Mukerji, Stanford University*
**pradhan1@stanford.edu*

Summary

We present a framework for efficiently performing 3D seismic inversion of reservoir facies under geologically realistic geostatistical models of prior uncertainty. Our approach is based on directly learning the inverse mapping between 3D seismic data and reservoir models using 3D convolutional neural networks. We generate training dataset for the learning problem by simulating facies from object-based geostatistical model and forward modeling seismic data. We present a method for performing falsification of prior geologic uncertainty with seismic data, which is critical to ensure reliability during prediction with real data. We demonstrate the efficacy of our approach by successfully inverting a large-scale model of a real deltaic reservoir from 3D post and partial stack seismic data.

Introduction

Building geologically realistic models of hydrocarbon reservoir facies is essential for reliable reservoir performance forecasting and decision-making. State-of-the-art geostatistical reservoir modeling approaches such as training image based, object-based, surface-based and process-based modeling (Pyrcz and Deutsch, 2014) have significantly extended our capabilities for capturing geologically complex reservoir facies architectures. However, reliably conditioning these modeling algorithms to dense geophysical data such as 3D seismic data by inverse modeling remains a key research challenge. In order to generate geologically realistic realizations of the earth, the afore-mentioned geostatistical algorithms are parameterized in terms of geological patterns, objects, surfaces or events. Integration of conventional geophysical inversion methods with such geological parameterization of the model space is non-trivial to accomplish. For instance, by parameterizing facies with surface-based models, the seismic response of the reservoir model will not vary continuously with respect to the model parameters. This restricts explicit usage of gradient-based optimization for solving the inverse problem (Bertoncello, 2011).

Monte Carlo sampling-based methods can potentially be employed to address these challenges. The general strategy is to generate samples by performing a stochastic exploration of the model space and forward modeling their data response. These samples are subsequently either accepted or rejected in accordance to a fitting criterion based on observed data. While most Monte Carlo methods are asymptotically guaranteed to converge to the target solution, computational costs can be significant even for low to moderately high dimensional model spaces. To boost computational tractability, special search strategies have been employed by several authors to guide the stochastic exploration towards important regions of the model space. Grana et al. (2012) and Jeong et al. (2017) employ the probability perturbation method and adaptive spatial resampling respectively to boost efficiency of stochastic seismic inversion of facies. A limitation is that such search strategies are typically tailored to specific geostatistical models and methodological modifications might be required if a different model is employed. A solution to this issue is to re-parameterize the geological prior model using another model which is more amenable to integration with conventional stochastic optimization methods. Nesvold (2019) and Mosser et al. (2020) propose learning object-based geostatistical representation with generative adversarial networks. Mosser et al. (2020) further demonstrate how the re-parameterization facilitates usage of a conventional Markov chain Monte Carlo based optimization method to sample the posterior distribution. Such an approach entails additional computational costs as it is required to sample the geological prior to create a training set, optimize a machine learning model to re-parameterize the geological model and finally perform stochastic optimization for data conditioning.

In this paper, we propose to employ deep learning to directly learn the inverse functional relationship linking seismic data to facies. To make predictions with this approach, a single optimization problem, for training the deep learning model, needs to be solved. Modern deep learning models can be trained by gradient-based optimization methods, which are significantly faster than stochastic optimization methods. Deep learning has been adopted for addressing various geophysical inverse and interpretation problems in recent years (Wu et al., 2019, Yang and Ma, 2019; Das et al., 2019; Pradhan and Mukerji, 2020). The contribution of the present paper is that it demonstrates how 3D CNNs can be employed to efficiently accomplish 3D seismic inversion of facies under geologically realistic prior uncertainty. Our proposed methodology consists of specifying object-based prior uncertainty on facies and performing unconditional simulations to generate multiple realizations of the reservoir model. Subsequently, seismic forward modeling is performed to generate corresponding seismic responses. The simulated facies and seismic realizations serve as the

training dataset for solving a statistical classification problem. Note that the proposed approach is flexible regarding the nature of the geostatistical model since the sole requirement is the ability to perform unconditional simulations with this model. However, it is imperative to use a statistical learning model that can encapsulate the complex geological and geophysical rules and interactions exhibited by the training dataset. For this purpose, we employ deep 3D convolutional neural networks (CNNs), which have been shown to successfully capture highly abstract and non-linear representations in spatially dense prediction tasks (Long et al., 2015).

We apply our methodology to a real case study from a producing gas reservoir from offshore Nile delta. We will be performing our analysis on an area having a spatial extent of 5 kms along x and y directions. Structural interpretations of the reservoir top and base horizons were available to us. The minimum depth to reservoir top is 2100 meters and the reservoir zone has an average thickness of 250 meters. The reservoir grid was discretized into 100, 100 and 250 cells along x, y and depth dimensions. Available seismic data consisted of 3D time migrated post stack volume, near stack volume obtained by stacking 2^0, 7^0 and 12^0 angle gathers and far stack volumes obtained from 21^0, 26^0 and 30^0 angle gathers. Figure 1 shows these volumes on the seismic grid with 100, 100 and 75 cells along x, y and time dimensions. The seismic data has a dominant frequency of 15 Hz. Petrophysical logs from seven wells were available. Three wells were kept completely blind throughout the analysis for validation purposes. Using this dataset, we demonstrate how 3D CNNs can be employed to efficiently perform a 3D inversion of reservoir facies model from seismic data.

Modeling of prior geologic uncertainty

The first component of our methodology is to specify and sample the prior geological uncertainty model on facies to generate multiple facies realizations. Prior geomorphological analyses in the study area (Cross et al., 2009) have interpreted the presence of channels with splays, leveed channels and thin beds in reservoir zone. Correspondingly, we specify six facies for the reservoir model: gas saturated channels, brine saturated channels, splays, levees, background shale and thin beds. Prior facies uncertainty is parameterized using object-based geostatistical representation. Object-based models require specification of parameters controlling the shape and geometry of each facies object. We assigned probability distributions for these parameters based on prior knowledge available regarding geology (Cross et al., 2009) of the study area. In Table 1, we show the probability distributions (pdfs) for channel geo-object parameters. Similar pdfs were used to assign prior uncertainty on all other facies parameters. Object-based simulations were performed under this prior model to generate 2400 facies model realizations (Figure 2). We assumed the prior for gas-water contact (GWC) depth to follow a triangular distribution with lower and upper limits of 2415 and 2450 meters respectively, based on water saturation logs available at the wells. For every facies realization, the GWC depth value is sampled from its prior to separate the channel objects further into gas or brine saturated channels. Note that while the geological model contains six different facies, we will perform the seismic inversion for three facies: gas sands, brine sands and non-reservoir facies. Splays, levees, thin beds and shales were lumped together into non-reservoir facies as analysis of elastic logs at the wells showed significant overlap between the elastic properties of the above four facies. This indicates that seismic data will not be able to resolve these non-reservoir facies from each other.

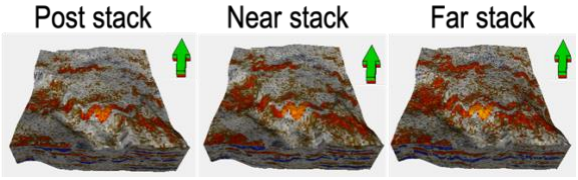

Figure 1: Post stack, near stack and far stack seismic data in the study area. The seismic grid is 5x5 km with average time thickness of 0.23 seconds

Table 1: Probability distributions on parameters controlling geometry of sinusoid channel geo-objects. $\mathcal{N}(\mu, \sigma)$: Gaussian distribution; $\mathcal{T}(a, b, c)$: triangular distribution.

Geo-object	Parameters	Distributions
Channel	Global proportion	$\mathcal{N}(33\%, 8\%)$ Upper limit = 0, Lower limit = 70%
Channel	Amplitude	$\mathcal{T}(300m, 400m, 500m)$
Channel	Wavelength	$\mathcal{T}(350m, 600m, 800m)$
Channel	Width	$\mathcal{T}(100m, 250m, 450m)$
Channel	Thickness	$\mathcal{T}(2m, 15m, 30m)$
Channel	Orientation	$\mathcal{T}(240^0, 305^0, 310^0)$

Elastic property and seismic modeling

The next step is to generate corresponding realizations of elastic properties and forward model seismic volumes. Prior uncertainty on P-wave velocity (v_p), S-wave velocity (v_s) and bulk density (ρ_b) are specified using multi-Gaussian distributions based on log data. Variograms for v_p, v_s and ρ_b were modeled separately for each facies using the sonic, shear-sonic, bulk density and petrophysical facies interpretation logs available at four wells. Sequential Gaussian simulation (Deutsch and Journel, 1992) was employed to generate 2400 realizations of v_p, v_s and ρ_b. Figure 2 shows two realizations for v_p and v_s. Subsequently, 2400 realizations of post-stack, near stack and far stack synthetic seismic data were generated using single-scattering forward modeling with the full nonlinear Zoeppritz equations and angle-dependent wavelets

extracted using seismic-well ties. In Figure 2, we show two realizations of post-stack seismic data. To account for modeling imperfections and data noise, we add random noise to all seismic realizations with signal-to-noise ratio sampled from a uniform distribution with lower and upper limits of 0.5% and 30% noise respectively.

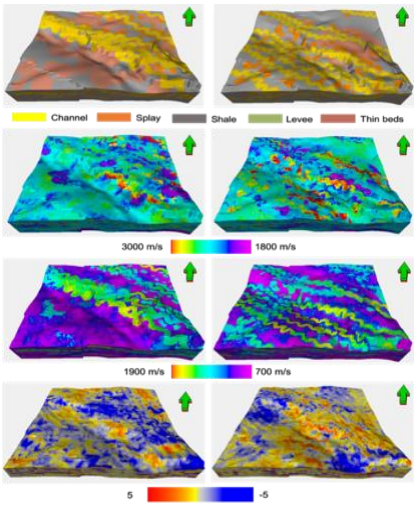

Figure 2: Two 3D realizations (out of 2400) of facies, P-velocity, S-velocity and post-stack seismic amplitudes (from top to bottom).

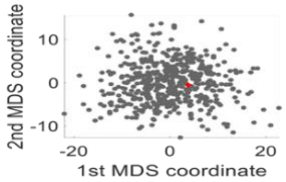

Figure 3: Prior realizations of post-stack seismic data (in gray) and real seismic data (red) plotted in two MDS coordinates

Falsification of prior uncertainty with seismic data

A critical component of our proposed methodology is to perform falsification of the prior uncertainty model (Scheidt et al., 2017; Pradhan and Mukerji, 2020). Since specification of the prior geological model is subjective, a possibility is that the real data might be statistically inconsistent with simulated synthetic data. A deep learning model trained on such inconsistent training dataset cannot be expected to make robust predictions with real data. Falsifying the geological prior corresponds to establishing whether the geological patterns present in the real seismic data belong to the same statistical population as patterns captured by the object-based model. For this purpose, we employ a global pattern matching methodology proposed by Scheidt et al., 2015. We perform the falsification analysis with post-stack seismic responses of 500 prior models. Specifically, 3D wavelet decomposition is performed for 500 randomly selected (out of 2400) post-stack seismic realizations along with the real post stack seismic. Subsequently, we compute mutual distances between the seismic volumes using global histograms of wavelet coefficients as proposed by Scheidt et al. (2015). Using this dissimilarity measure, the realizations are projected into a 2-dimensional space using multi-dimensional scaling (MDS; Borg and Groenen, 1997) as shown in Figure 3. It can be ascertained visually that, in MDS space, the real seismic data belongs to the same population as modeled seismic realizations. The prior is thus not falsified, and a deep learning model trained with the synthetic training set can be used for making predictions with real data.

Inverse modeling with 3D CNNs

We employ 3D CNNs to learn the inverse mapping from seismic data to facies. The CNN takes as input the post-stack, near-stack and far-stack seismic cubes, stacked as a 4D tensor of dimensions $\mathbf{75 \times 100 \times 100 \times 3}$. The first and last dimensions correspond to time and stacking-type of seismic data. Details of the CNN architecture is shown in Table 2. The CNN outputs the probability of each facies class at each cell of the reservoir grid. The output has dimensions $\mathbf{250 \times 100 \times 100 \times 3}$. The first and last dimensions correspond to depth and facies type respectively. For training the CNN, the simulated 2400 realizations were divided into training, validation and test sets containing 2000, 200 and 200 realizations respectively. The network was trained for 100 epochs (~ 48 hours run time) with Adam optimizer (Kingma and Ba, 2015) on a machine with 128 GB RAM and two 32GB Tesla V100 GPUs.

Table 2: Details of the CNN architecture. 'Conv3D' refers to 3D convolutional layers. Batch normalization layers were used after every convolutional layer

Layer type	Filter size	# of filters	Conv type	Strides	Dilation factor	Activation	Output shape
Input							75×100×100×3
Conv3D	3×3×3	32	Same	1×1×1	1×1×1	RELU	75×100×100×32
Conv3D	3×3×3	32	Same	1×1×1	1×1×1	RELU	75×100×100×32
Transposed Conv3D	26×1×1	32	Valid	1×1×1	1×1×1	RELU	100×100×100×32
Conv3D	3×3×3	32	Same	1×1×1	2×2×2	RELU	100×100×100×32
Conv3D	3×3×3	32	Same	1×1×1	4×4×4	RELU	100×100×100×32
Transposed Conv3D	52×1×1	32	Valid	2×1×1	1×1×1	RELU	250×100×100×32
Conv3D	3×3×3	32	Same	1×1×1	8×8×8	RELU	250×100×100×32
Conv3D	3×3×3	32	Same	1×1×1	16×16×16	RELU	250×100×100×32
Conv3D	3×3×3	32	Same	1×1×1	32×32×32	RELU	250×100×100×32
Conv3D	3×3×3	3	Same	1×1×1	1×1×1	Sigmoid	250×100×100×3

To evaluate the training quality, most likely facies models are derived from the CNN predicted facies probabilities and compared against the true models in the training, validation and test sets. We obtained mean pixel-wise classification accuracies of 88.1%, 87.8% and 88.4% respectively for training, validation and test sets. High classification accuracy on the test set models evidences good

generalization of the trained CNN to unseen examples. In Figure 4, we compare the true facies against CNN predictions along a depth and cross-section from a test set model. It can be observed how the CNN has almost perfectly learned to predict the complex geometries of the channel objects. The CNN has predicted the spatial locations of the channels and GWC with high accuracy. This indicates that the CNN has learnt a robust inverse mapping from seismic to facies while honoring the geological rules present in the geostatistical prior model.

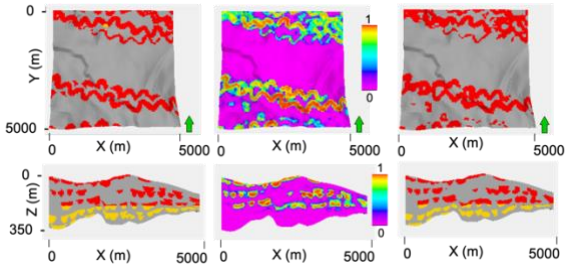

Figure 4: CNN prediction results for a test set model. Depth-sections (top row) and cross-sections (bottom) of true facies (left column), predicted gas sand probability (middle column) and predicted most likely facies (right column). Gas sands are shown in red, brine sands in yellow and non-reservoir facies in gray.

Previous analysis of test set results indicated that the network is not overfitting to training data and thus can be used for predictions with real dataset. The acquired post-stack, near-stack and far-stack volumes are input to the CNN to make predictions. In Figure 5, we present results along a depth and cross-section of the reservoir grid. As expected from test set results, the CNN has preserved the geologic continuity of the channelized features evident in the seismic amplitude section. We further validate the predictions by comparing the predicted gas sand probabilities against the gamma ray log and legacy facies petrophysical facies interpretations at two wells in Figure 6. The CNN has successfully predicted the gas sand intervals in both wells with high probability.

Conclusions

Solving a 3D seismic inverse problem for reservoir facies under geologically realistic prior uncertainty can be methodologically and computationally very challenging. In this study, we proposed direct learning of the inverse mapping with 3D CNNs as an efficient approach to address these challenges. Using a real case study of an off-shore deltaic reservoir, we demonstrated the efficacy of our approach by estimating a reservoir model with 2.5 million grid cells from 3D post and partial stack seismic data.

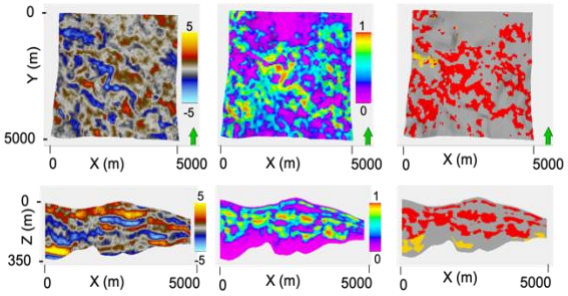

Figure 5: CNN prediction results from real seismic data. Depth-sections (top row) and cross-sections (bottom) of depth converted post-stack real seismic (left column), predicted gas sand probability (middle column) and predicted most likely facies (right column). Gas sands are shown in red, brine sands in yellow and non-reservoir facies in gray.

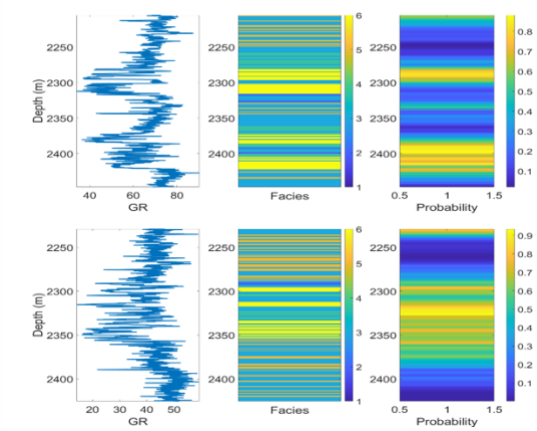

Figure 6: Gamma ray log (left column), legacy petrophysical interpretations (middle column; 1: brine sand, 2: splay, 3: shale, 4: levee, 5: thin bed, 6: gas sand) and CNN predicted gas sand probability (right column) at well 1 (top row) and blind well 2 (bottom row). Gas sands are in yellow.

Acknowledgements

This work is supported by the sponsors of the Stanford Center for Earth Resources Forecasting (SCERF). We would also like to thank Steve Graham, the Dean of the School of Earth, Energy, and Environmental Sciences at Stanford University for funding. We thank Edison E&P for providing the dataset used in this study. We offer special thanks to Giuseppe Bellentani, Francesco Siliprandi and Luca Di Cesare for their help and advice regarding the real dataset.

References:

Bertoncello, A., 2011, Conditioning surface-based models to well and thickness data: Ph.D. Thesis, Stanford University.

Borg, I., and P. Groenen, 1997, Modern Multidimensional Scaling: Theory and Applications. Springer.

Cross, N. E., A. Cunningham, R. J. Cook, A. T. E. Esmaie, N. E. Swidan, 2009, Three-dimensional seismic geomorphology of a deep-water slope-channel system: The Sequoia field, offshore west Nile Delta, Egypt. *AAPG Bulletin* ; 93 (8): 1063–1086, doi: https://doi.org/10.1306/05040908101

Das, V., A. Pollack, U. Wollner, and T. Mukerji, 2019. Convolutional neural network for seismic impedance inversion. Geophysics 84 (6), 1–66.

Deutsch, C., A. G., Journel, 1992, GSLIB: geostatistical software library and user's guide. Oxford University Press, London.

Grana, D., T. Mukerji, J. Dvorkin, G. Mavko, 2012, Stochastic inversion of facies from seismic data based on sequential simulations and probability perturbation method. Geophysics. 77(4), M53–M72, https://doi.org/10.1190/geo2011-0417.1

Jeong, C., T. Mukerji, and G. Mariethoz, 2017, A Fast Approximation for Seismic Inverse Modeling: Adaptive Spatial Resampling. Math Geosci, 49, 845–869, https://doi.org/10.1007/s11004-017-9693-y

Kingma, D., and J. Ba, 2014, Adam: a method for stochastic optimization: arXiv preprint arXiv:1412.6980

Long, J., E. Shelhamer, and T. Darrell, 2015, Fully convolutional networks for semantic segmentation, CVPR.

Mosser, L., O. Dubrule, and M. J. Blunt, 2020, Stochastic Seismic Waveform Inversion Using Generative Adversarial Networks as a Geological Prior. Math Geosci 52, 53–79, https://doi.org/10.1007/s11004-019-09832-6

Nesvold, E., 2019, Building informative priors for the subsurface with generative adversarial networks and graphs: Ph.D. Thesis, Stanford University

Pradhan, A., and T. Mukerji, 2020, Seismic Bayesian evidential learning: estimation and uncertainty quantification of sub-resolution reservoir properties: Computational Geosciences, https://doi.org/10.1007/s10596-019-09929-1

Pyrcz, M. J., and C. V. Deutsch, 2014, Geostatistical Reservoir Modeling, Oxford University Press, Oxford.

Scheidt, C., C. Jeong, T. Mukerji, and J. Caers, 2015, Probabilistic falsification of prior geologic uncertainty with seismic amplitude data: Application to a turbidite reservoir case, Geophysics 80: M89-M12.

Scheidt, C., L. Li, J. Caers, 2017, Quantifying uncertainty in subsurface systems. Wiley-Blackwell, New Jersey.

Wu, X., L. Liang, Y. Shi, and S. Fomel, 2019, FaultSeg3D: Using synthetic data sets to train an end-to-end convolutional neural network for 3D seismic fault segmentation, Geophysics 84: IM35-IM45.

Yang, F., and J. Ma, 2019, Deep-learning inversion: A next-generation seismic velocity model building method, Geophysics 84: R583-R599.